FY-2016 Methyl Iodide Higher NO_x Adsorption Test Report

Fuel Cycle Technology

Prepared for
U.S. Department of Energy
Material Recovery and Waste Form Development Campaign

Nick Soelberg
Tony Watson
Idaho National Laboratory
September 29, 2016

FCRD-MRWFD-2016-000352
INL/EXT-16-40087

ACKNOWLEDGEMENTS

The authors acknowledge others who helped guide or perform methyl iodide adsorption testing this year. Jack Law of the Idaho National Laboratory (INL) and Bob Jubin of the Oak Ridge National Laboratory provided programmatic and technical direction. Cathy Rae in the INL Chemistry and Radiation Measurement Department performed gas chromatography with mass spectrometry analyses. Duane Ball and Paula Hahn in the INL Chemistry and Radiation Measurement Department performed iodine sample analyses. Amy Welty of the INL Aqueous Separations and Radiochemistry Department assisted with data reduction.

This page blank

SUMMARY

Nuclear fission produces fission and activation products, including iodine-129, which could evolve into used fuel reprocessing facility off-gas systems, and require off-gas control to limit air emissions to levels within acceptable emission limits.

Deep-bed methyl iodide adsorption testing has continued in Fiscal Year 2016 under the Department of Energy (DOE) Fuel Cycle Technology (FCT) Program Offgas Sigma Team to further research and advance the technical maturity of solid sorbents for capturing iodine-129 in off-gas streams during used nuclear fuel reprocessing.

Adsorption testing with higher levels of NO (approximately 3,300 ppm) and NO_2 (up to about 10,000 ppm) indicate that high efficiency iodine capture by silver aerogel remains possible. Maximum iodine decontamination factors (DFs, or the ratio of iodine flowrate in the sorbent bed inlet gas compared to the iodine flowrate in the outlet gas) exceeded 3,000 until bed breakthrough rapidly decreased the DF levels to as low as about 2, when the adsorption capability was near depletion.

After breakthrough, nearly all of the uncaptured iodine that remains in the bed outlet gas stream was no longer in the form of the original methyl iodide. The methyl iodide molecules are cleaved in the sorbent bed, even after iodine adsorption is no longer efficient, so that uncaptured iodine was in the form of iodine species soluble in caustic scrubber solutions, and detected and reported as diatomic I_2.

The mass transfer zone depths were estimated at 8 inches, somewhat deeper than the 2-5 inch range estimated for both silver aerogels and silver zeolites in prior deep-bed tests, which had lower NO_x levels.

The maximum iodine adsorption capacity and silver utilization for these higher NO_x tests, at about 5-15% of the original sorbent mass, and about 12-35% of the total silver, respectively, were lower than for trends from prior silver aerogel and silver zeolite tests with lower NO_x levels.

Additional deep-bed testing and analyses are recommended to expand the database for organic iodide adsorption and increase the technical maturity if iodine adsorption processes.

This page blank

TABLE OF CONTENTS

LIST OF FIGURES

LIST OF TABLES

ACRONYMS AND ABBREVIATIONS

AgA	silver aerogel
DF	decontamination factors
DL	detection limit
DOE	Department of Energy
DOG	dissolver off-gas
ECD	electron capture detector
EDS	energy dispersive spectroscopy
FCT	Fuel Cycle Technology
FID	flame ionization detector
FP	fission product
FY	fiscal year
GC	gas chromatograph
GCMS	gas chromatography with mass spectrometry
ICPMS	inductively coupled plasma mass spectrometry
INL	Idaho National Laboratory
MTZ	mass transfer zone
SEM	scanning electron microscopy
SPME	solid-phase micro-extraction

This page blank

1. INTRODUCTION

The Department of Energy (DOE) Fuel Cycle Technology (FCT) Program Offgas Sigma Team has supported research and development on iodine control and iodine waste forms for the past several years. This research and development has included iodine adsorption tests using multiple-segmented fixed beds of Ag-laden iodine adsorbents. Tests thus far in this "deep-bed" system have been done using NO_x concentrations on the order of up to 2,000 ppm. Tests done during this fiscal year were performed with higher NO_x concentrations of over 10,000 ppm, to determine the performance of iodine sorbents with a gas mixture that more fully represents the possible range of dissolver off-gas (DOG) NO_x concentrations, which could range up to several percent (Law 2015).

All work was performed in compliance with work control documentation that was updated in fiscal year (FY) 2014 to ensure data quality, worker safety, environmental protection, and regulatory compliance during testing (INL 2015).

2. DEEP BED IODINE SORBENT TEST SYSTEM

Figure 2-1 shows a process diagram for the iodine test system. The test system consists of the following main components:

- Process gas supply and blending system, which supplies gases from gas cylinders, gas generators, and a humidifier
- Multiple sorbent bed system inside a heated oven
- Process gas bypass
- Inlet and bed segment outlet gas sampling system.

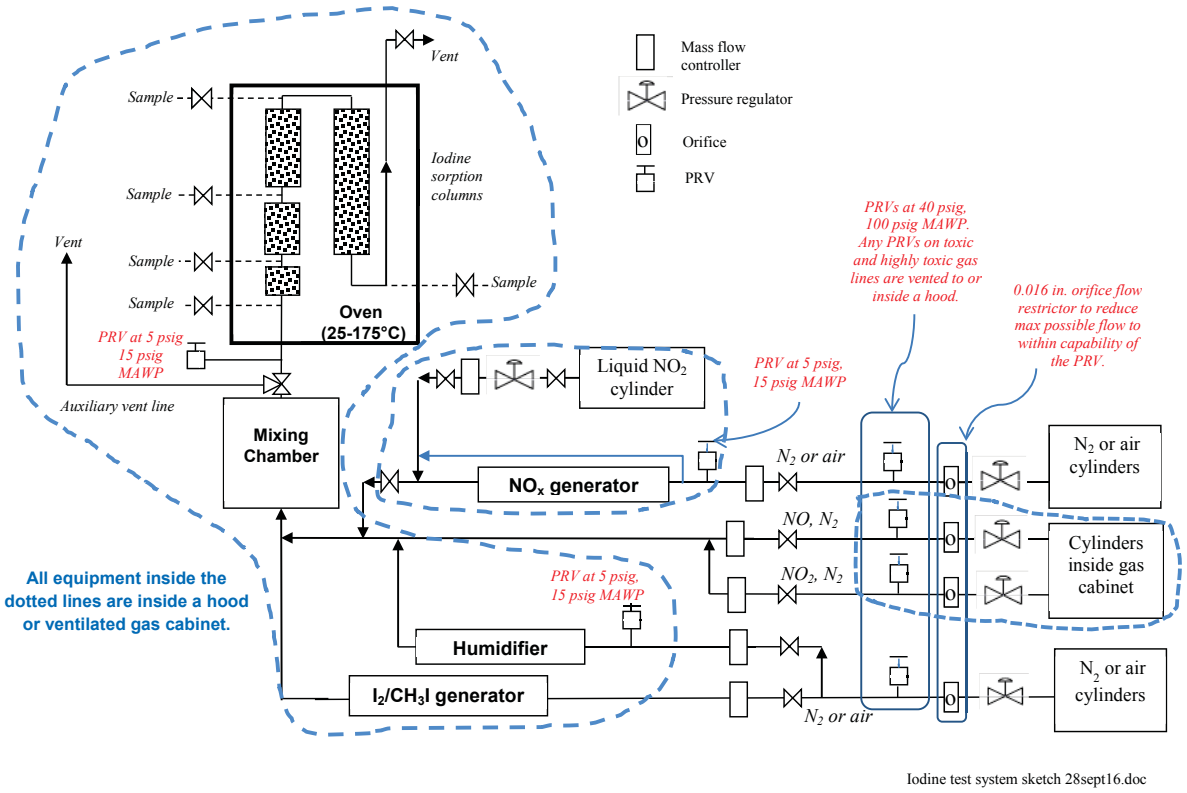

Figure 2-1. Deep-bed adsorption test system.

2.1 Process Gas Supply System

The process gas supply system consists of pressurized gas cylinders and gas generator systems that supply the gases that are blended together to make the gas mixture that is passed through the sorbent beds. These gases can include (depending on the test) pure air, nitrogen, NO, NO_2, water vapor, diatomic iodine, and methyl iodide (as a surrogate for organic iodide). Air or N_2 can be supplied through mass flow controllers separately to the iodine and methyl iodide generators, the humidifier, and the NO_2 generator. NO and NO_2 gases, with balance N_2, are supplied from compressed gas cylinders through mass flow controllers. An NO_2 generator system supplies higher NO_2 concentrations than can be provided from compressed gas.

Methyl iodide and iodine gases are provided using compressed gas cylinders, permeation tubes, or a fixed bed iodine generator. The choice of methyl iodide and iodine source depends on the flowrate needed to achieve the target concentration in the test gas mixture. For lower methyl iodide concentrations under about 1 ppm, compressed gas cylinders or a permeation tube system are used. For low iodine concentrations, under about 2 ppm, or for methyl iodide concentrations above about 1 ppm, the permeation tube system is used. For higher iodine concentrations, above about 2 ppm, a fixed bed of iodine crystals interspersed in glass beads (which prevents iodine crystal agglomeration) is used.

The permeation tube system uses semi-permeable tubes that contain liquid methyl iodide (or solid iodine crystals) to emit a known flowrate of methyl iodide (or iodine) at a constant rate, which is controlled by the operating temperature of the tube. The tubes (up to two), from VICI Metronics, are

placed inside a Dynacalibrator Model 190 constant temperature permeation tube system (Figure 2-2) also from VICI Metronics.

The gas flowrates and the generation rates of vaporized iodine, methyl iodide, and water are set to achieve the target gas composition and blended in a mixing chamber upstream of the sorbent beds. All process lines that contain vaporized iodine, methyl iodide, or water are electrically heat traced.

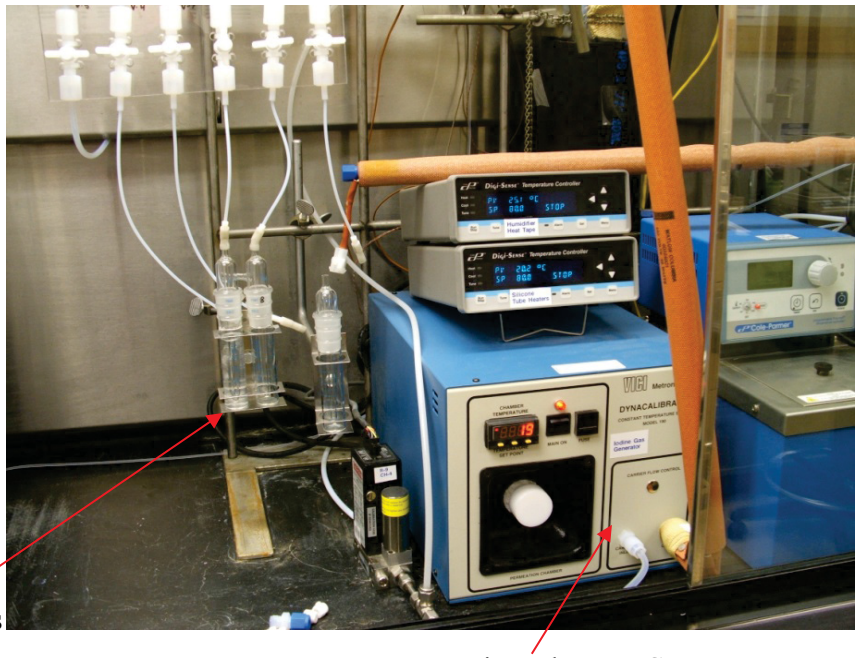

Figure 2-2. View of the iodine impingers and the permeation tube iodine or methyl iodide generator.

Humidified air is produced by passing air or nitrogen through a fritted glass bubbler submerged in a constant temperature water bath. A thermocouple in the headspace of the bubbler provides the temperature of the water-saturated gas. The concentration of water in the blended gas is controlled by adjusting the gas flowrate through the humidifier and the humidifier operating temperature.

2.2 NO_2 GENERATOR SYSTEM

From the recent Case Study (Law 2015) and based on results of dissolver off-gas testing by Birdwell 1991, benchmark total NO_x levels in the dissolver off-gas stream downstream of a recycling condenser have been estimated at 1 volume %, of which NO is 30% (3,000 ppm) and NO_2 is 70% (7,000 ppm) of the total NO_x. Deep-bed iodine adsorption testing has not yet included evaporated HNO_3, though there is a potential for evaporated HNO_3 in the dissolver off gas (DOG) downstream of the condenser.

The amount of NO_2 that can be provided in compressed gas cylinders is limited for the size of this bench-scale test system because higher NO_2 concentrations in N_2 are pressure-limited, and higher gas cylinder pressures have limited NO_2 concentrations. It is not practical or cost-effective to use compressed gas cylinders of NO_2 for long-duration deep-bed iodine adsorption testing with NO_2 levels greater than about 1,000 ppm in gas streams at flowrates up to about 1 L/min.

The NO_2 generator system (Figures 2-3 and 2-4) evaporates liquid N_2O_4 to produce gaseous NO_2 for blending with the other gas streams that comprise the gas mixture for deep-bed iodine adsorption tests. In this system, the liquid N_2O_4 cylinder is mildly heated to no higher than 50°C (the safe operating limit for the cylinder) to create sufficient pressure in the cylinder (Figure 2-5) and provide heat for vaporizing the N_2O_4 and the endothermic conversion of N_2O_4 to NO_2. Second, the conversion of gaseous N_2O_4 dimer to NO_2 is assured by heating the gas stream to about 150°C, which is the nominal operating temperature of the sorbent test bed system. At this temperature, the equilibrium constant for the conversion of N_2O_4 to NO_2 favors NO_2 (Figure 2-6) and facilitates NO_2 flowrate monitoring and control.

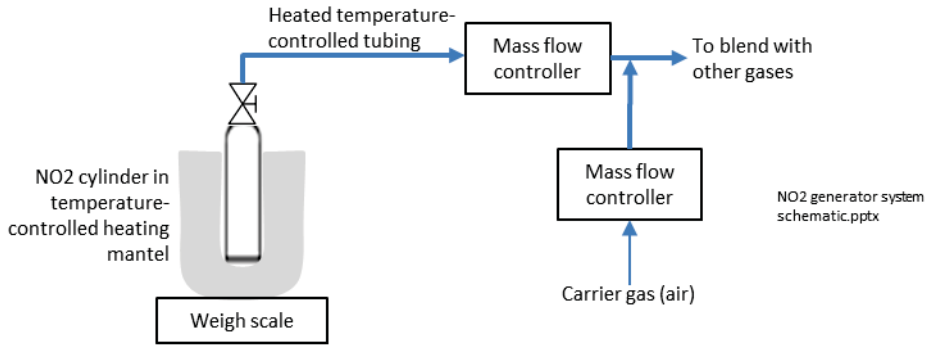

Figure 2-3. NO_2 generator system schematic.

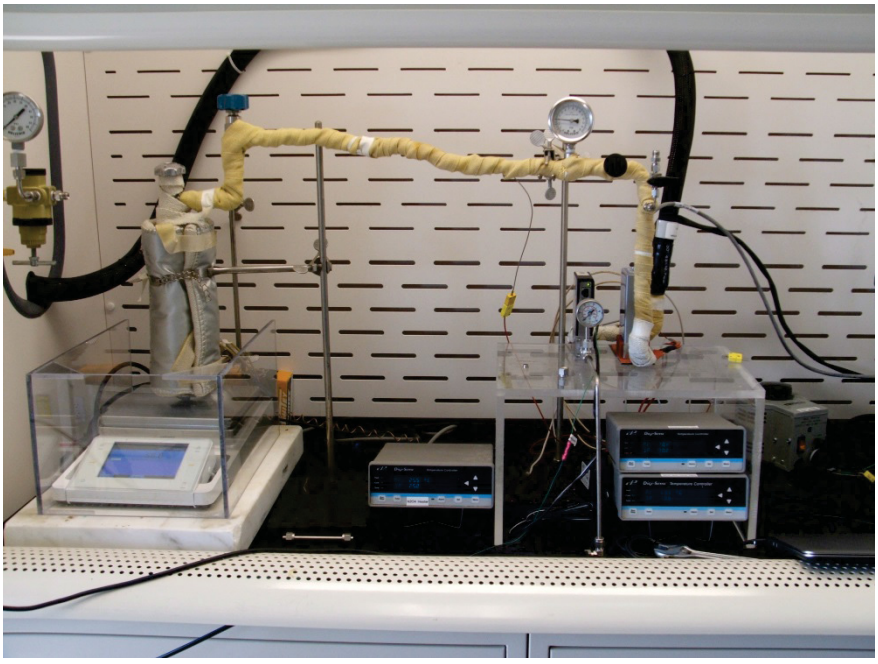

Figure 2-4. Photograph of the NO_2 generator system.

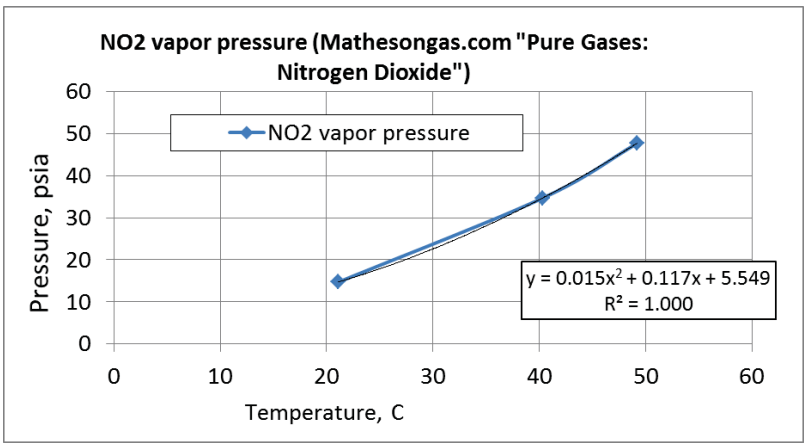

Figure 2-5. NO_2 vapor pressure.

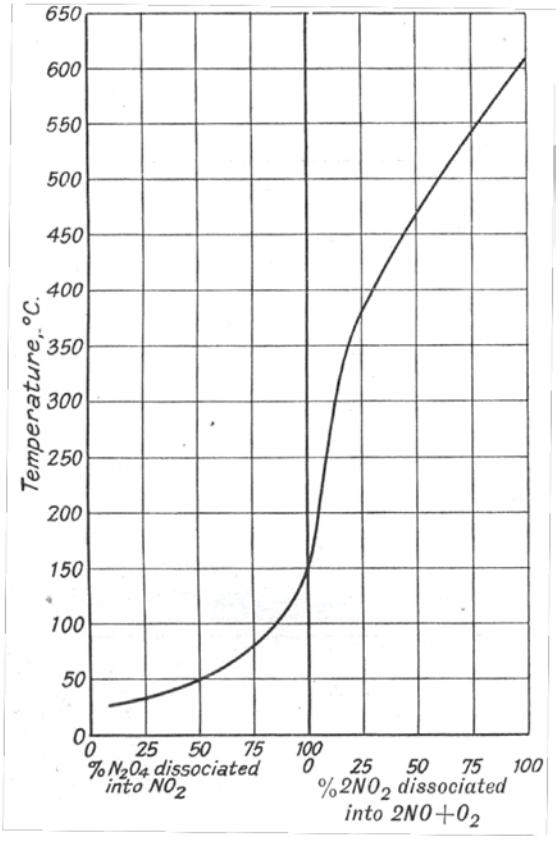

Figure 2-6. N_2O_4 and NO_2 dissociation equilibria (http://nitrogen.atomistry.com/nitrogen_tetroxide.html).

Initial testing indicated that the mass flow controller could not accurately control the NO_2 gas flowrate, due to the uncertainty in the conversion of the gasified N_2O_4 to NO_2 at the operating temperature of about 60°C for the mass flow controller. While the mass flow controller managed the instantaneous

NO_2 flowrate, the actual time-averaged NO_2 flowrate was measured gravimetrically by weight change of the N_2O_4 cylinder.

The NO_2 gas is promptly blended, after flowrate control, with the carrier gas (Figure 2-5) to lower the NO_2 concentration and prevent condensation. This blend of NO_2 and carrier gas is then mixed with the rest of the gas mixture to be used in deep-bed iodine adsorption testing.

2.3 Sorbent Bed Segments

Figures 2-7 and 2-8 show detail of the sorbent beds and how the sorbent beds are configured in a temperature-controlled oven. The current test design includes up to four sorbent bed segments. The sorbent bed segments are made of borosilicate glass. A glass frit at the bottom of each bed segment supports the granular sorbent.

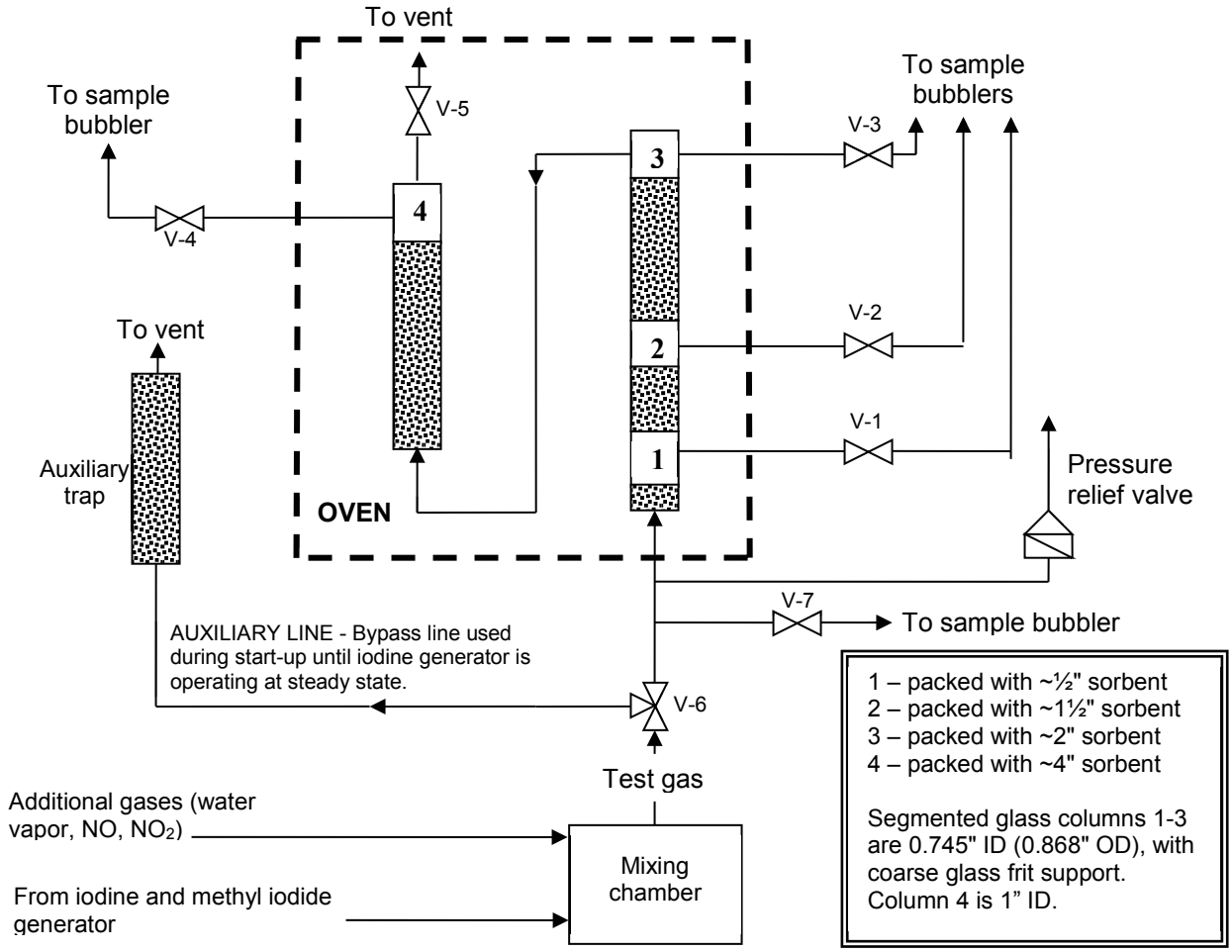

Figure 2-7. Detail of the sorbent beds.

Figure 2-8. Configuration of the sorbent beds inside the temperature-controlled oven.

2.4 Sample Collection and Analysis

Iodine and methyl iodide concentrations in the test gas can be measured at up to five locations in the test system – at the inlet to the sorbent bed segments, and at the outlet of each of up to four bed segments. Since the gas flowrate is essentially the same at all five sample locations, the removal efficiencies for the sorbent in all four beds can be determined by measuring the iodine and methyl iodide concentrations at these locations.

The iodine loadings and silver utilizations can be determined by several methods including (a) integration over time differences in the gaseous iodine concentrations for a given flowrate, (b) sorbent pre- and post-test gravimetric measurements, or (c) measurement of silver and adsorbed iodine using analytical methods such as scanning electron microscopy energy dispersive spectroscopy (SEM/EDS) or using wet chemistry methods of sorbent digestion followed by sample analysis. Using these methods for many tests has shown that the SEM/EDS method can provide the most reliable and quickest results. The SEM/EDS method, while subject to some experimental error, is not subject to (a) cumulative increasing experimental error observed in the gas analysis method, (b) experimental error in the gravimetric method due to relatively small weight changes and the potential for bias if the sorbent weight changes for other reasons such as the desorption or adsorption of other species, or (c) experimental error when portions of the sorbent are not completely digested prior to analysis.

2.4.1 Iodine Sample Collection and Analysis

Iodine measurements are made even when iodine is not included in the test gas mixture to determine if, or how much, iodine is being formed from reactions of methyl iodide.

For measuring the gaseous iodine concentration, the process gas from any of the five sample locations is passed through 25-ml "midget" impingers that contain 0.3 M NaOH for scrubbing halogen gases, including I_2 and HI, if present. This technique is modeled after EPA Method 26 "Determination of Hydrogen Halide and Halogen Emissions from Stationary Sources, Non-Isokinetic Method" (40 CFR 60

Appendix A). The caustic solution scrubs the halogens by hydrolyzing halogen gases to form a proton (H^+) and hypohalous acid.

Any HI, if present, dissociates into the caustic solution, and is included with I_2 in the analysis. Therefore, this test method does not discriminate between I_2 and HI or other iodine species that are soluble in 0.3 M NaOH.

The bubbler solutions are analyzed by inductively coupled plasma mass spectrometry (ICPMS) per EPA Method 6020A (SW-846, "Test Methods for Evaluating Solid Wastes Physical/Chemical Methods," http://www.epa.gov/osw/hazard/testmethods/sw846/online/). The gaseous iodine detection limit (DL) is about 0.08 ppb with this method. Higher-concentration samples for gas streams with 1 ppm or higher iodine concentrations are typically diluted for analysis.

2.4.2 Organic Compound Sampling and Analysis

Methyl iodide analysis using gas chromatography (GC) has evolved over time due to the corrosive nature of the typical test gas. Early testing used a Hewlett-Packard model 5890 Series II gas chromatograph (GC) installed in-line with the sample loop, thereby allowing near real-time analysis of methyl iodide [Haefner 2010]. An Rt-Q-BOND fused silica capillary column was used in the GC. The GC was equipped with an electron capture detector (ECD), which is very sensitive for measuring halogenated organic compounds. The minimum DL for this GC setup was about 5 ppb.

This early testing indicated that the use of the sample loop (which enables frequent and automatic sampling) and the highly sensitive ECD resulted in apparent corrosion of GC components resulting in erroneous measurements. The GC was frequently down for maintenance. Essentially all components that contacted the sample gas were eventually replaced, and the GC continued to frequently malfunction.

Beginning in FY-2013, the GC was replaced with another Hewlett Packard 5890 GC, equipped with a RTX-624, 30 m x 0.32 mm ID, 1.8 µm df column, and a flame ionization detector (FID). The sample loop was not used. This caused the sampling and analysis to be more operator time-intensive, and reduced the number of GC measurements that are practical, but reduced the amount of time that the GC components are exposed to the corrosive sample gas.

The FID is not as sensitive for methyl iodide analysis as the ECD. The methyl iodide DL is about 1 ppm using direct injections. When lower DLs are desired, then a solid-phase micro-extraction (SPME) syringe is used. A SPME adsorbs organic compounds onto a solid-phase sorbent in a needle, thereby concentrating the amount of analyte. The adsorbed analytes are then desorbed into the GC carrier gas at an elevated temperature.

The SPME syringe is a Supelco brand, containing 75 µm carboxen/polydimethylsiloxane fiber. The SPME and GC are calibrated together for specified adsorption and desorption times and temperatures. Using a SPME improves the methyl iodide DL for the FID by approximately 100x to approximately 10 ppb.

Unknown organic compounds formed by reactions of methyl iodide can appear as additional peaks on the GC-FID chromatograms. When this occurs, they can be tentatively identified using gas chromatography with mass spectroscopy (GCMS) analysis. The GCMS used for this work is a Shimadzu GC2010 with GCMS-QP2010 (with autosampler). The column is a J&W Scientific DB-1 (dimethyl polysiloxane) column, 30 m x 0.25 mm ID x 1 µm df.

3. DEEP BED METHYL IODIDE TEST RESULTS

Methyl iodide testing proceeded, consistent with the joint methyl iodide test plan (Jubin 2015) except that silver aerogel (AgA) was used as the sorbent instead of silver zeolite, in order to expand the AgA

sorbent data base. Two long-duration adsorption tests for CH_3I on AgA were completed this fiscal year. Table 3-1 summarizes the results of these tests. The target CH_3I concentration in the gas stream was 50 ppm; the target NO and NO_2 concentrations were 3,300 ppm and 10,000 ppm respectively. The moisture content was nominally 0.60 volume %, corresponding to a dewpoint of 0°C.

Table 3-1. Results of the long-duration methyl iodide test.

Run Number	CH3I-17 High NOx Ag Aerogel	CH3I-18 High NOx Ag Aerogel
Simulate what off-gas?	Dissolver	Dissolver
Test start date	1-Jun-16	8-Aug-16
Sorption conditions		
Temperature, deg. C	150	150
Total gas flowrate, L/min	0.72	0.73
Target bed inlet CH3I conc, ppmv	50	50
Average measured bed inlet CH3I conc, ppmv	47	65
Average measured bed inlet I2 conc, ppmv	0.28	0.46
H2O conc, %	0.60%	0.59%
H2O dewpoint, deg. C	0	0
NO conc., ppmv	3,326	3,268
NO2 conc., ppmv	5,682	9,635
Balance	air	air
Sorption gas velocity, m/min	4.3	4.4
Depths of each successive orbent bed, inches	0.5, 1, 2.5, 4	0.5, 1, 2.5, 4
Cumulative sorbent bed depths, inches	0.5, 1.5, 4, 8	0.5, 1.5, 4, 8
Bed 1 out residence t, sec	0.13	0.13
Bed 2 out cumulative residence t, sec	0.45	0.44
Bed 3 out cumulative residence t, sec	0.89	0.88
Bed 4 out cumulative residence t, sec	2.32	2.28
AgA Ag concentration from SEM/EDS, wt%	30.5%	30.5%
AgA weight change, %	1.8%	-3.5%
Cumulative test duration, hrs	179	314
Iodine loadings from SEM/EDS	% adsorbed iodine of mass of initial sorbent	
Bed 1	14.9%	5.0%
Bed 2	7.6%	4.2%
Bed 3	7.2%	2.7%
Bed 4	No detect	2.8%
Silver utilization, %		
Bed 1	35%	12%
Bed 2	16%	10%
Bed 3	16%	6.9%
Bed 4	No detect	7.7%
Max DF before breakthrough	7,494	3,509
Average conversion of CH3I to I2 in inlet gas	1.2%	1.4%
Max conversion of bed outlet CH3I to I2	100%	100%
Mass transfer zone depth, inches	8	8
Organic compounds tentatively identified	None could be identified	

iodine data 26sept16.xlsx]2016 summary

Silver aerogel prepared by Pacific Northwest National Laboratory was the sorbent, with a silver content of 30.5 wt%, as measured by SEM/EDS.

The degree to which the CH_3I in the inlet gas stream was converted to other iodine species via gas-phase reactions, prior to entering the sorbent bed segments, was determined by sampling the inlet gas stream for iodine species soluble in 0.3 M NaOH, such as HI or I_2. Analysis of the scrub solutions indicated less than 1% of the inlet CH_3I converted to HI/I_2.

Figure 3-1 shows the sorbent in the sorbent beds prior to adsorption testing. The virgin sorbent was dark-colored >0.85 micron-sized particles comingled with a few lighter colored particles. The maximum particle size was 1-2 micron.

Figure 3-2 shows how the first, shallower beds change color first, as the iodine chemisorbs, or as gas constituents or reaction products of methyl iodide decomposition adsorb on or otherwise react with the sorbent. As the dark sorbent color fades, the sorbent takes on a greenish tinge.

Figure 3-3 shows the sorbent at the end of the 179-hr long CH3I-17 test and purge. A post-test purge, intended to desorb and remove any weakly-held iodine, which was not chemisorbed on the sorbent was performed at the end of the test. The sorbent color became uniformly lighter shades of white and grey. The sorbent with the least amount of iodine adsorption, at the bottom of the down-flow fourth bed, had the least color-change, although it had also become considerably lighter, with a somewhat greenish tinge.

Figure 3-1. AgA sorbent in the sorbent beds prior to the test CH3I-17.

Figure 3-2. Sorbent beds 1 and 2 showing greenish and faded coloration compared to bed segment 4 which was still mostly dark colored, at about hour 80 in the CH3I-17 test, when the Bed 1 and 2 DFs were about 1.5 and 5, respectively, and the Bed 4 DF was about 100.

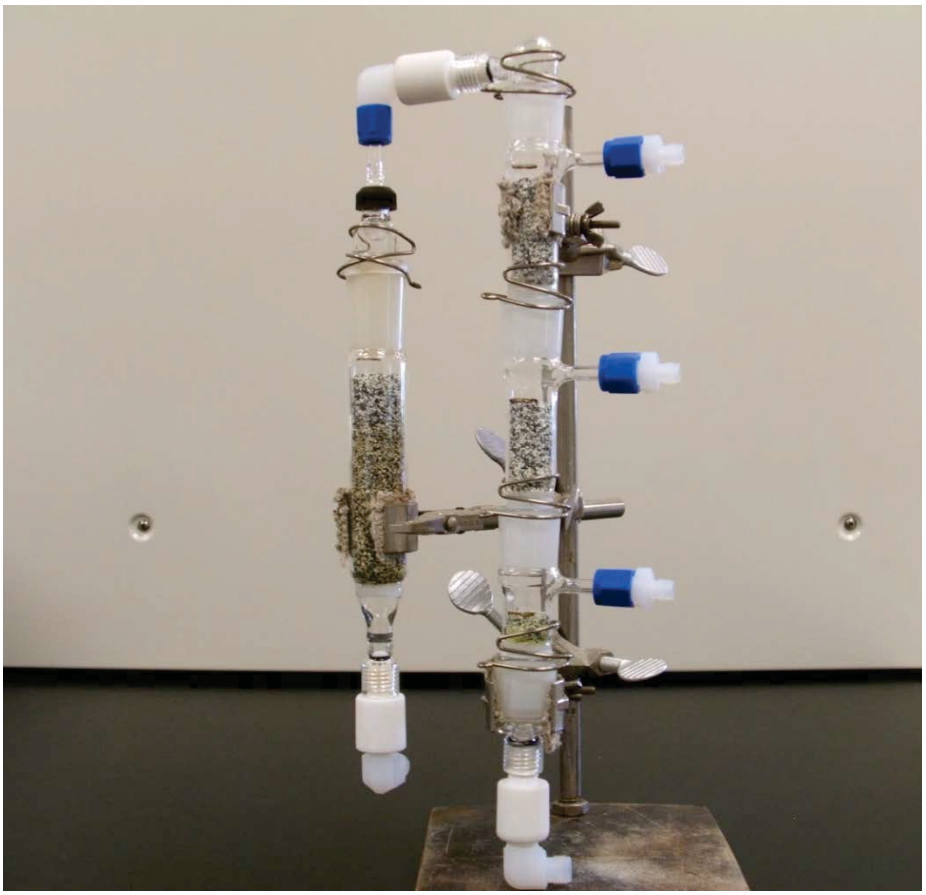

Figure 3-3. Iodine-laden AgA sorbent in the sorbent beds following the CH3I-17 test.

Figure 3-4 shows how the sorbent color faded after about hour 200 in the CH3I-18 test, which had about twice the NO_2 concentration as the CH3I-17 test had. The sorbent was even lighter-colored than the sorbent in the shorter-duration, lower-NO_2 CH3I-17 test. Figure 3-5 shows that the sorbent at the end of the CH3I-18 test was even lighter-colored.

Figure 3-4. Sorbent appearance after hour 200 during the CH3I-18 test.

Figure 3-5. Sorbent appearance after purge was complete at the end of the CH3I-18 test.

3.1 Sorbent Performance in the Long-Duration Tests

3.1.1 Test CH3I-17

The decreasing trend in the sorbent DF during this test period for all four sorbent bed segments is shown in Figure 3-6. The DF was calculated by accounting for iodine in CH_3I and also iodine detected in the NaOH scrubbers. At the beginning of the test, the highest measured DF was over 7,000. The Bed 1 outlet DF, at only a 0.5 inch depth in the bed, decreased faster than for the other bed segment outlets. The outlet DFs of beds 2, 3, and 4 decreased soon after test startup, but stayed above about 3,000 for about 3.5 hours, when the DFs for these three beds all started decreasing at a faster rate. By hour 100, the DF at the outlet of Bed 2 matched the Bed 1 DF of about 1.5. By the end of the 179-hr test, the Bed 3 DF also nearly matched the DFs of Beds 1 and 2, although the Bed 4 DF had not yet decreased that far.

These DFs indicate that (a) the iodine adsorption mass transfer zone (MTZ) was about 8 inches deep (consistent with prior CH_3I test results [Soelberg 2014]) and (b) a deeper bed would be needed in a full-scale process to maintain DF levels that could be needed to meet regulatory requirements for longer than just a few hours. The DF trend shows that the adsorption capability for all four beds was depleted over time, as the CH_3I was reacted to release the iodine, which was adsorbed on the sorbent. The decrease in adsorption capability was fastest for Bed 1. The adsorption ability of Bed 1 decreased to near 0 (DF approaching 1) at about 60 hours into the test. The adsorption ability of Bed 4 decreased the slowest, decreasing to a DF of around 50 by the test end.

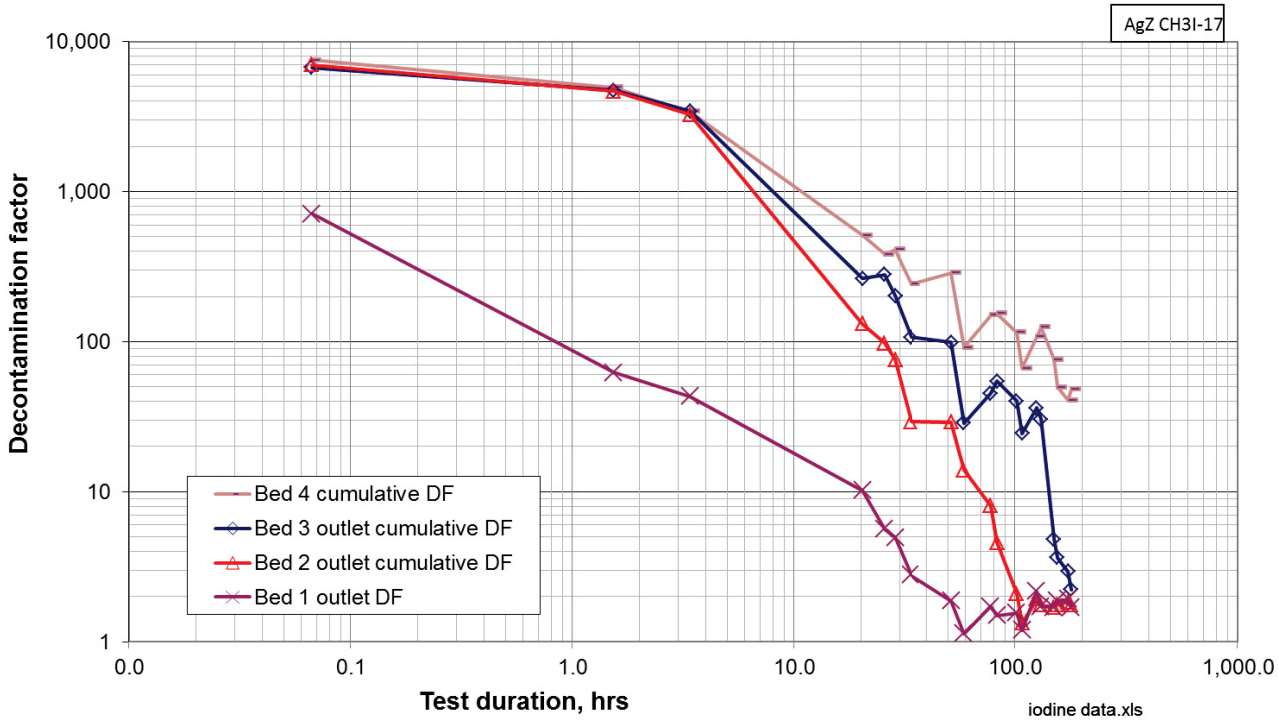

Figure 3-6. Total iodine DF trends over time for Test CH3I-17.

The CH_3I measurement trends are shown in Figure 3-7. This figure shows that initial bed outlet CH_3I concentrations were decreased by about three orders of magnitude for Bed 1 and about 5 orders of magnitude for the other, deeper bed segments. The bed outlet CH_3I concentrations increased for all four beds until between about hours 60 and 100, when the Bed 1, 2, and 3 outlet CH_3I concentrations appear to trend downward again. This did not occur in prior methyl iodide adsorption tests and may be a consequence of how the higher NO_x levels interact with the sorbent over time, and as the sorbent becomes more loaded with chemisorbed iodine.

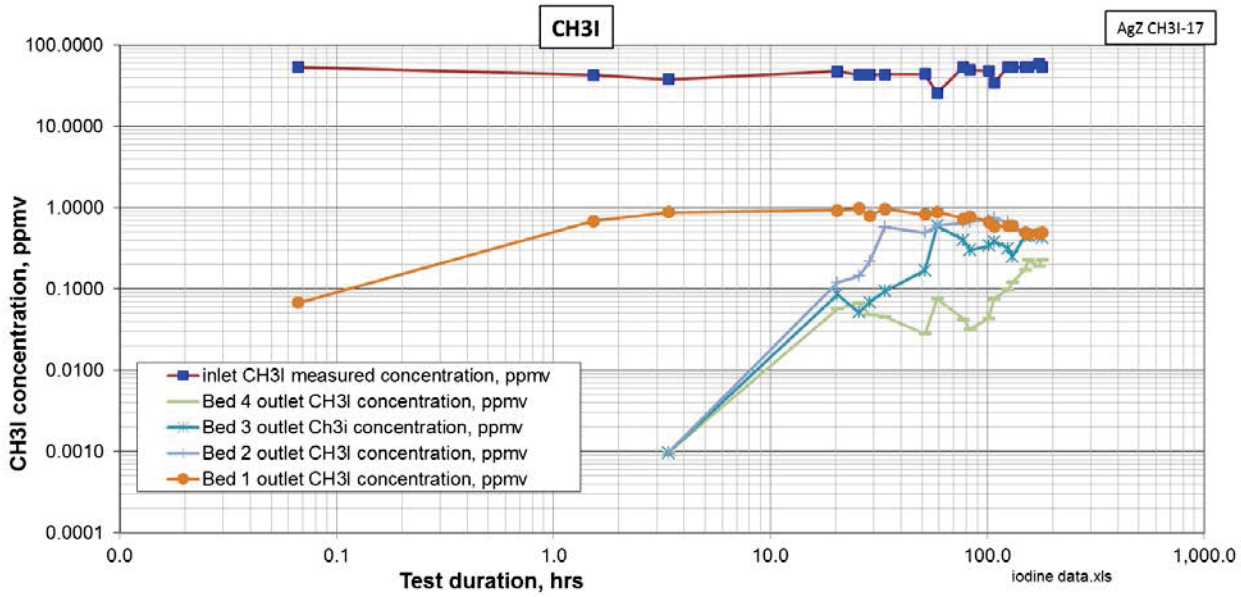

Figure 3-7. CH_3I concentration trends over time for Test CH3I-17.

The increase in bed outlet CH_3I concentrations was not the only, and not the major, contributor to the decreasing DFs. Figure 3-8 shows the increase in the measured iodine species detected in the NaOH scrub solutions, reported as I_2. The initial bed outlet I_2 concentrations were about four orders of magnitude lower than the inlet CH_3I concentrations, but gradually increased. The I_2 concentrations increased faster by about hour 2, with the Bed 1 I_2 concentrations increasing at the fastest rate, as is expected. By about hour 100 the Bed 1 and Bed 2 outlet I_2 concentrations reached a maximum of about 15 ppm and stopped increasing. By the test end, the Bed 3 outlet I_2 concentration also reached the ~15 ppm maximum.

These figures show that the major contributor to decreasing total iodine DFs was the formation of iodine species reported as I_2, not remaining CH_3I. Figure 3-9 shows the increasing trend in total unadsorbed iodine. In this figure, the diatomic I_2 concentration has been normalized to the monatomic iodine form, for direct comparison to the inlet CH_3I concentration. Chemical reactions occur as the gas mixture passes through the sorbent bed that break up the CH_3I; and allow adsorption of iodine, until the sorbent capability is depleted, at which time the unadsorbed iodine remains in the gas stream as iodine species that are soluble in NaOH solution. By test end, about 99.9% of the unadsorbed iodine is not CH_3I, but iodine species that are soluble in the NaOH scrubber solution.

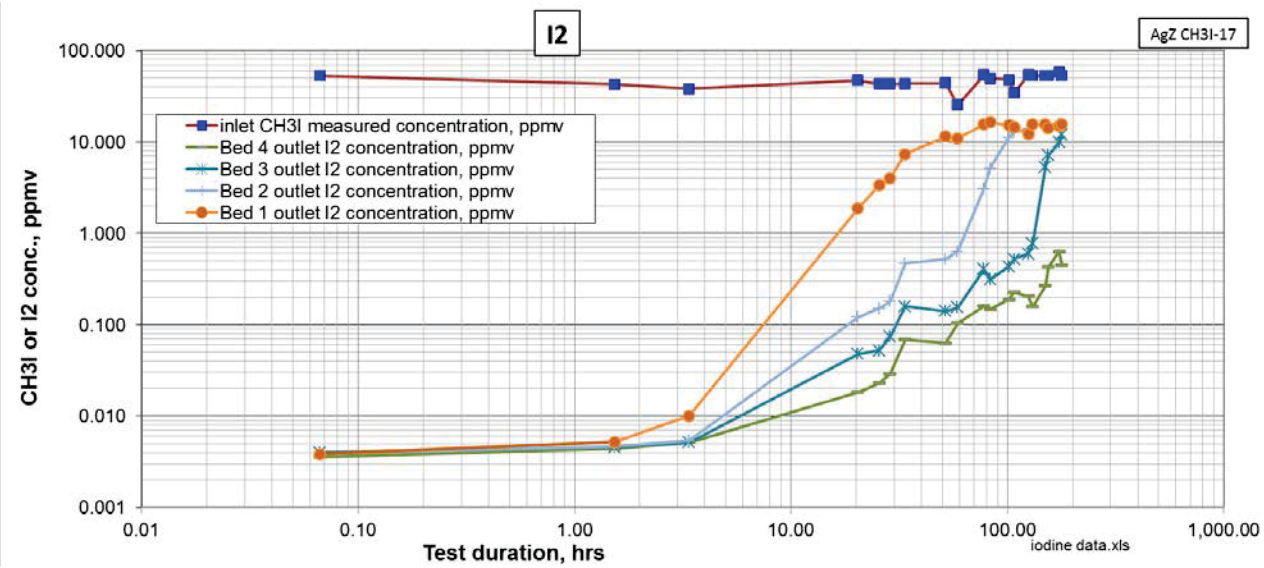

Figure 3-8. Bed segment outlet I_2 concentration trends over time for Test CH3I-17.

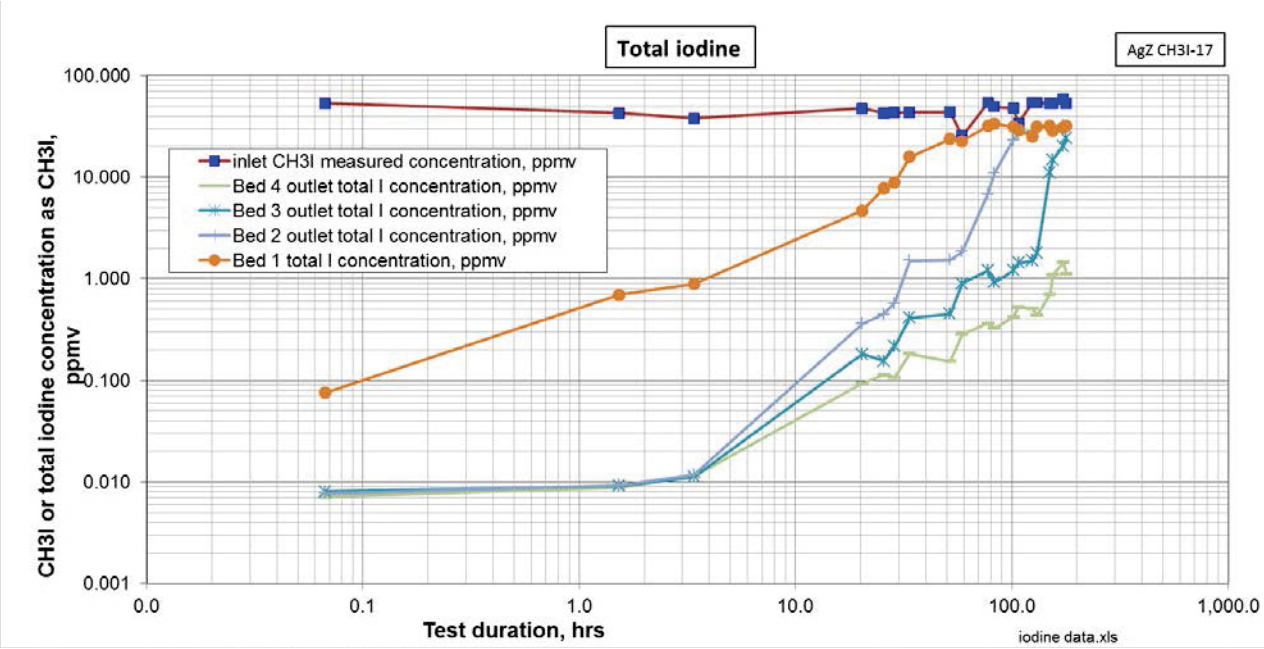

Figure 3-9. Bed segment outlet total iodine concentration trends over time for Test CH3I-17.

3.1.2 Test CH3I-18

The same sorbent performance trends observed in Test CH3I-17 are shown in Figure 3-10. At the beginning of the test, the highest measured DF was over 10,000. The Bed 1 outlet DF, at only a 0.5 inch depth in the bed, decreased faster than for the other bed segment outlets. The outlet DFs of beds 2, 3, and 4 decreased soon after test startup, but stayed above about 3,000 for about 4 hours, when the DFs for these three beds all started decreasing at a faster rate. By hour 80, the DF at the outlet of Bed 2 matched the Bed 1 DF of about 2. By the end of the 314-hr test, the Bed 3 and 4 DFs also nearly matched the Bed 1 and 2 DFs.

The mass transfer zone for these test conditions is also about 8 inches. The same adsorption reactions appear to prevail for these test conditions. The longer test duration allowed the DF for even the last bed segment to match the DFs for the other segments, indicating that the MTZ progressed well through the Bed 4 depth of 8 inches.

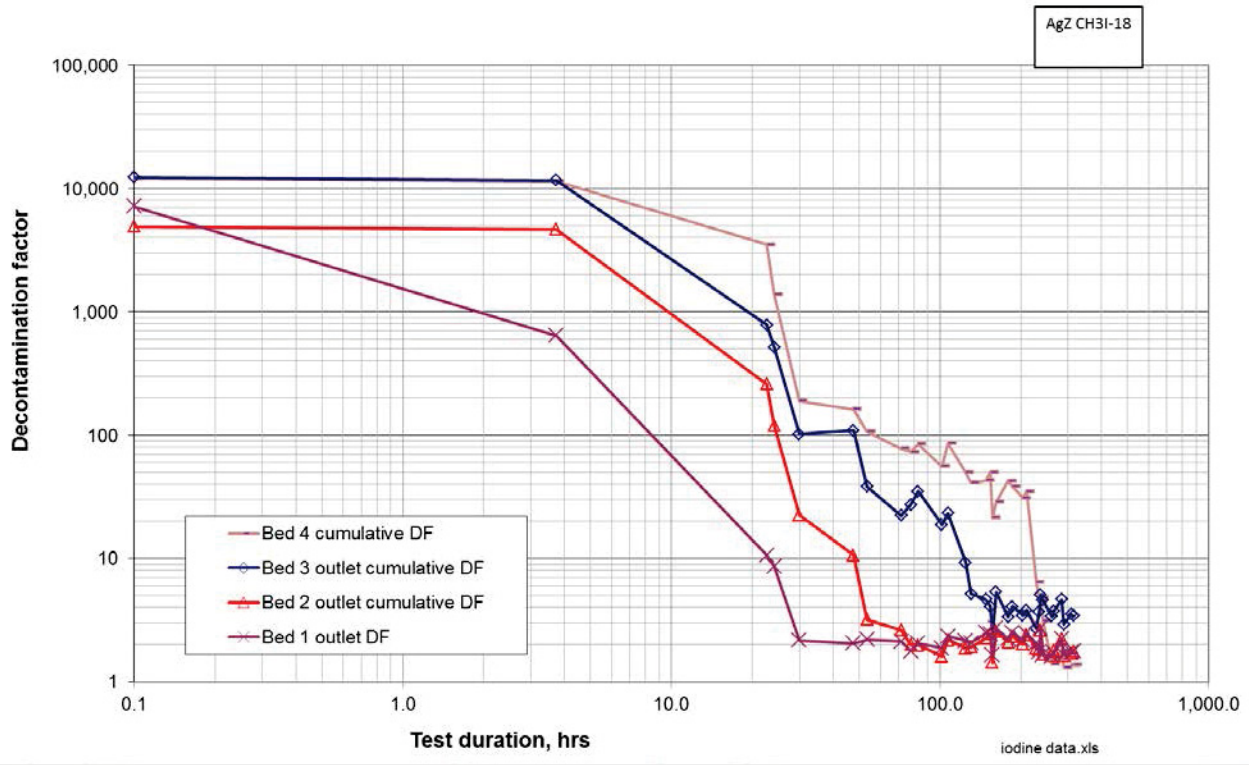

Figure 3-10. Total iodine DF trends over time for Test CH3I-18.

The bed outlet CH_3I concentrations shown in Figure 3-11 were not measureable until after hour 20, when the measured values increased enough to be above reporting limits of about 0.1 ppm for this test. Measured values prior to hour 20 were slightly negative, and were truncated to zero, and so do not show up on the log-long graph. Measured values increased for all four beds until between about hours 60 and 100, when the Bed 1, 2, and 3 outlet CH_3I concentrations appear to trend downward again. This is consistent with the CH_3I-17 test results, although it has not been noted in prior methyl iodide adsorption tests. It may be a consequence of how the higher NO_x levels interact with the sorbent over time, and as the sorbent becomes more loaded with chemisorbed iodine.

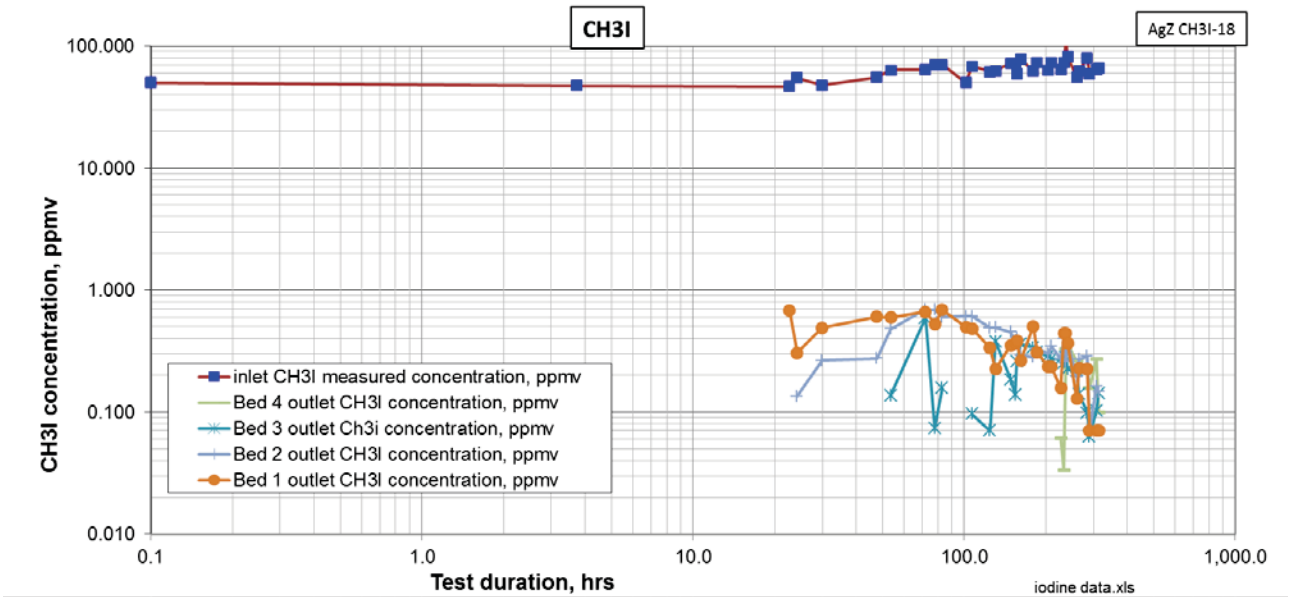

Figure 3-11. CH_3I concentration trends over time for Test CH3I-18.

Figure 3-12 shows the increase in the measured iodine species detected in the NaOH scrub solutions, reported as I_2. The same trends in bed outlet I_2 concentrations observed for the prior test are shown here. This test continued long enough so that the reported Bed 4 outlet I_2 concentration approximately matched the outlet concentrations for the other beds.

Figure 3-13 shows, like the prior test, the unadsorbed iodine reported as I_2 (not CH_3I) was the main contributor to the total unadsorbed iodine. By test end, about 99.9% of the unadsorbed iodine was not CH_3I, but iodine species that were soluble in the NaOH scrubber solution.

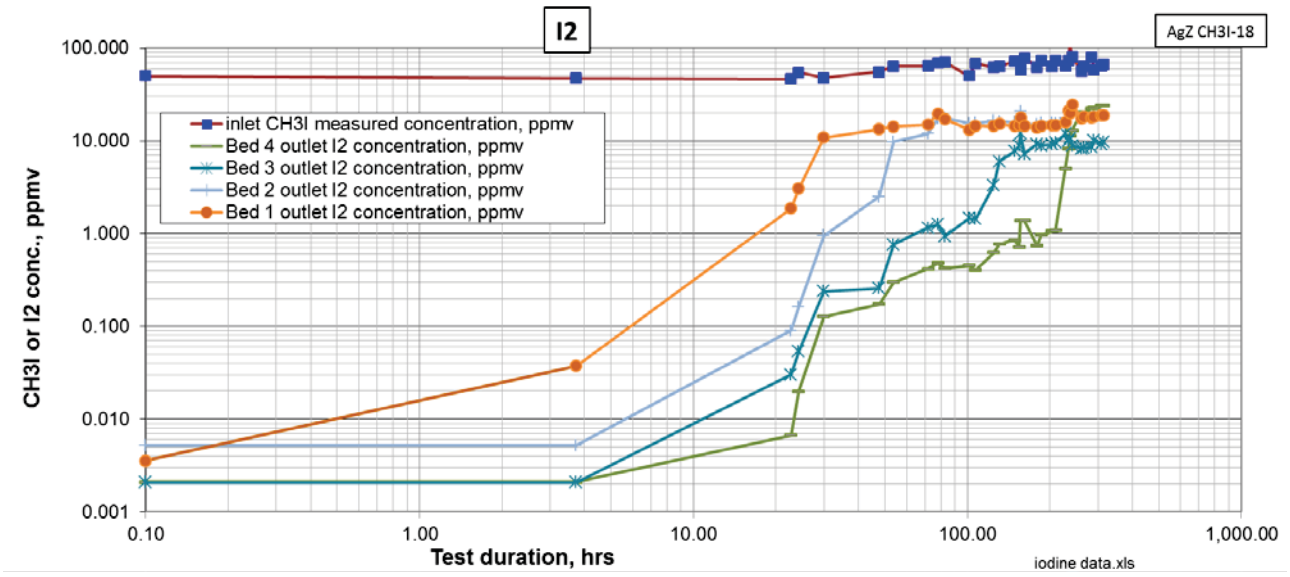

Figure 3-12. Bed segment outlet I_2 concentration trends over time for Test CH3I-18.

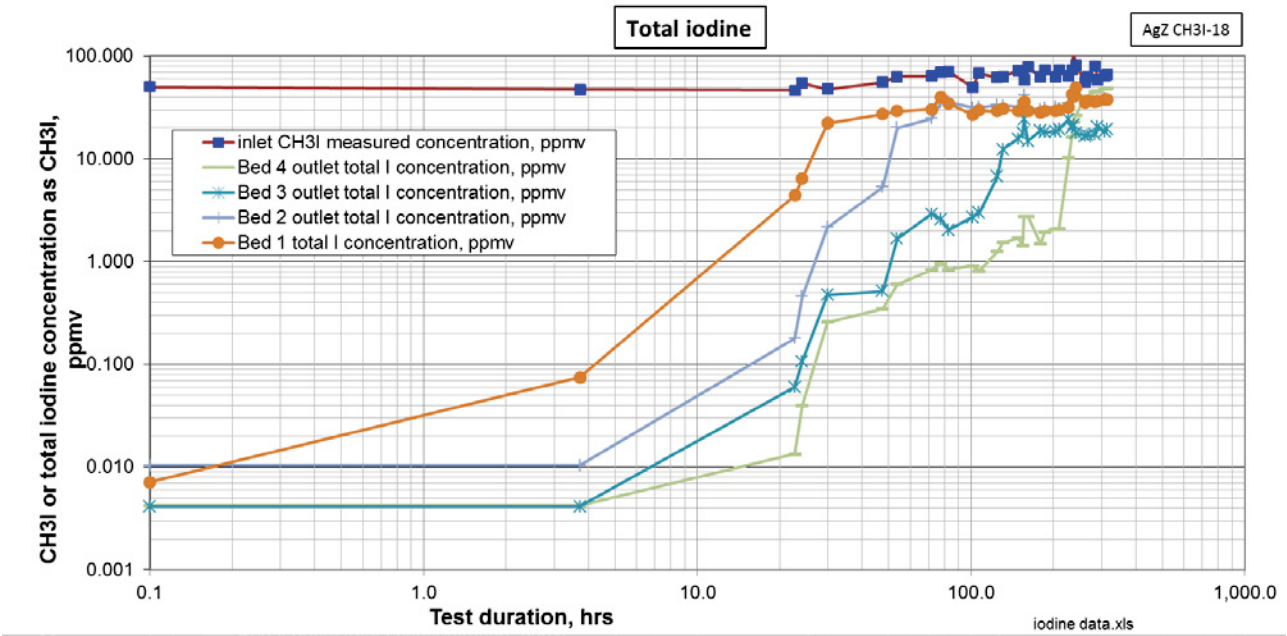

Figure 3-13. Bed segment outlet total iodine concentration trends over time for Test CH3I-18.

3.2 Sorbent Capacity

Figure 3-14 shows the post-test adsorbed iodine and silver utilization profiles for the sorbent. The iodine loading and silver utilization were determined using SEM/EDS measurements of silver and iodine concentrations in the virgin and spent sorbent. Since the iodine DFs did not reach 1 for either of these tests, even for the 0.5-in. deep Bed 1, these tests may not accurately indicate the maximum saturated capacity for iodine under the test conditions, which would be determined only after impractically long test durations.

Results of these tests are compared to other prior deep-bed iodine adsorption tests in Figure 3-15. The maximum iodine loadings and silver utilizations in Bed 1 for these tests were lower than has observed in other tests, perhaps due to the higher NO_x levels or due to incomplete saturation. However, many of the prior deep-bed tests, like these tests, also did not reach full iodine saturation in Bed 1.

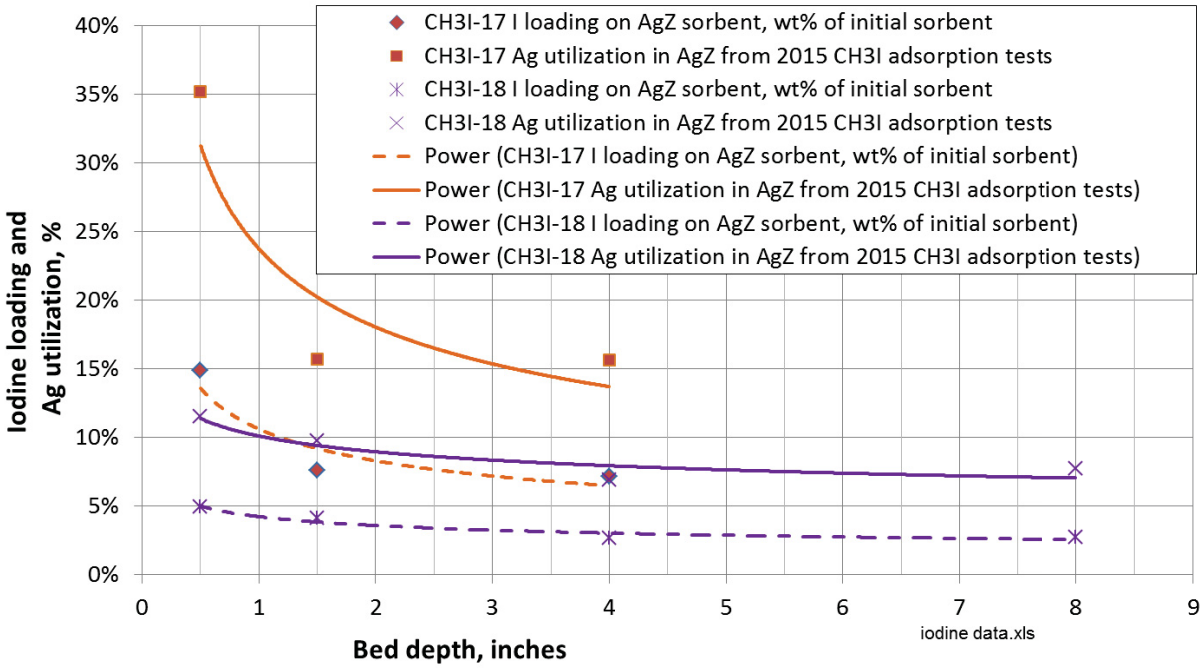

Figure 3-14. Iodine capacity and Ag utilization on AgA sorbent for the higher NO_x test conditions.

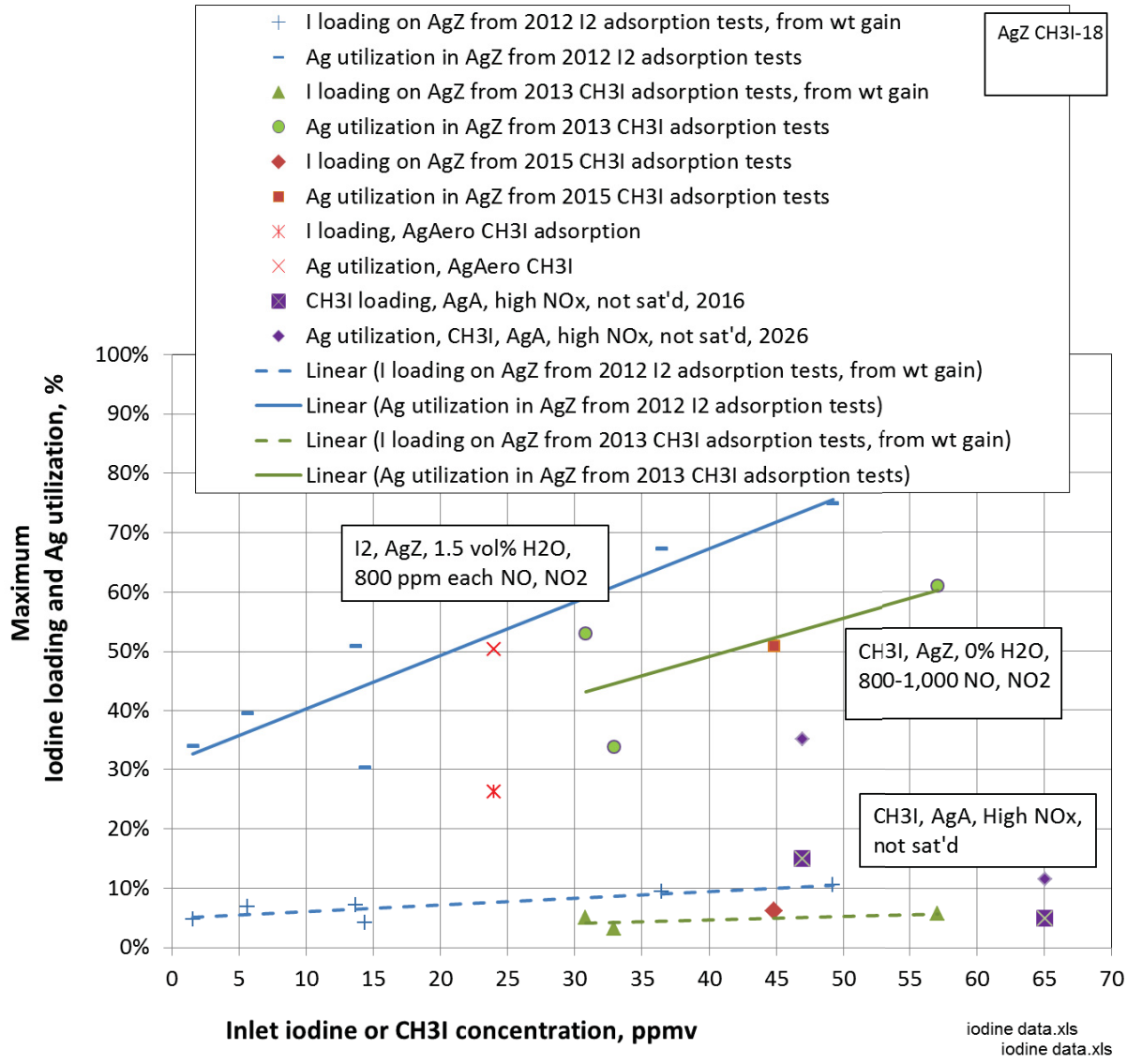

Figure 3-15. Iodine capacity and Ag utilization results from recent deep-bed tests.

3.3 Byproduct Species in the Sorbent Bed Outlet Gas

The GC-FID chromatograms of the bed segment outlet gas for these tests showed several peaks in addition to the CH_3I peak. Peaks detected in the samples of gas from the bed outlets were periodically analyzed by GCMS in attempts to tentatively identify these organic compounds. The GCMS was not as sensitive for these organic compounds as was the GC-FID, so some peaks detected on the GC-FID chromatograms were not detected by the GCMS.

An unusual feature of these higher NO_x tests was that, even after test progression long after DFs were reduced to under 10, the residual CH_3I in the bed outlet gas remained under 1 ppm, only around 2% maximum of the inlet CH_3I concentrations. The concentrations of other organic species detected in the GC-FID analysis were not high enough to enable detection and quantification by GCMS. Perhaps the

higher NO_x conditions were too reactive to allow for the formation of appreciable levels of organic byproduct compounds detected in prior, lower-NO_x tests (Soelberg 2015).

3.4 Post-Test Purging

After the test, the sorbent beds were purged to desorb any amounts of iodine that may be loosely held or physisorbed. The purge results for these tests are shown in Figures 3-16 and 3-17. These figures show that only a small fraction of the iodine sorbed on Bed 1 (about 0.1%) desorbed during the purge periods.

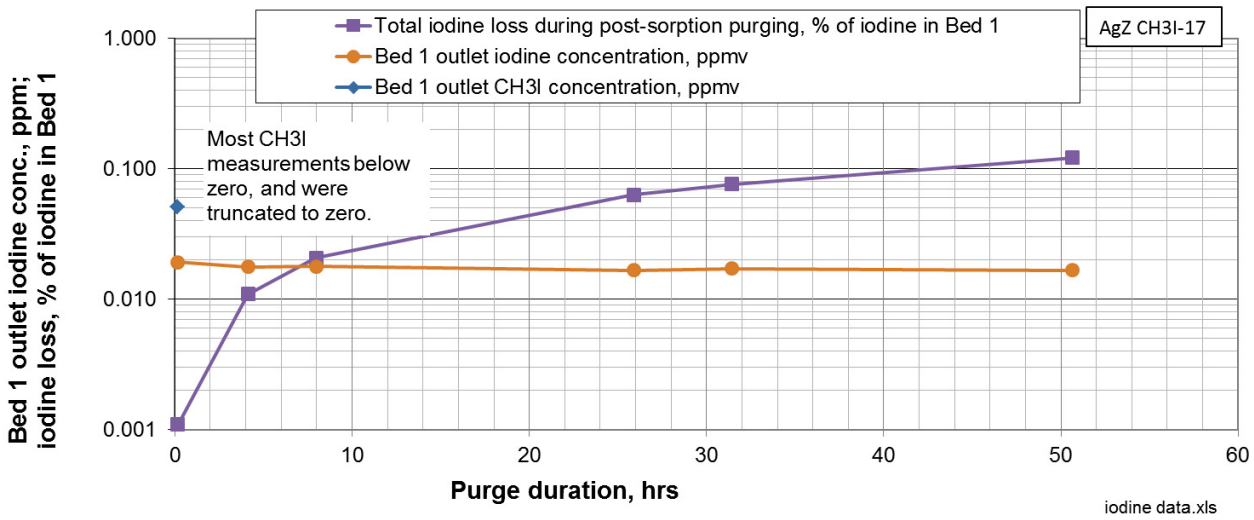

Figure 3-16. CH_3I-17 post-test sorbent purge results.

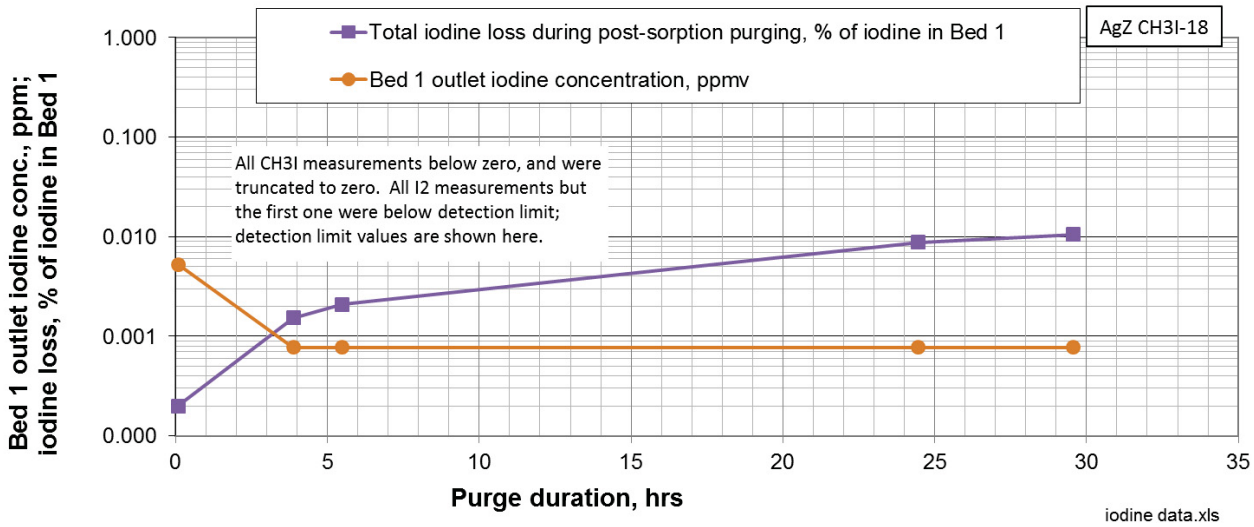

Figure 3-17. CH_3I-18 post-test sorbent purge results.

4. CONCLUSIONS AND RECOMMENDATIONS

Two deep-bed methyl iodide adsorption tests have been performed with higher NO_x levels, consistent with the recently updated multi-laboratory methyl iodide adsorption test plan [Jubin 2015]. High (>3,000) iodine DFs were achieved with the silver aerogel sorbent, although chemisorption capacities and silver utilizations appear to be lower than trends seen in prior deep-bed tests with lower NO_x levels. The iodine adsorption mass transfer zone for these tests was estimated at 8 inches, which is higher than estimated mass transfer zone depths for adsorption of I_2 under lower-NO_x conditions.

Additional deep-bed testing and analyses are recommended to expand the database for organic iodide adsorption and increase the technical maturity if iodine adsorption processes.

5. REFERENCES

Birdwell 1991 Birdwell, J.F., 1991, Iodine and NOx Behavior in the Dissolver Off-gas and IODCX Systems in the Oak Ridge National Laboratory Integrated Equipment Test Facility, NUREG/CP—011-Vol.1, Proceedings of the 21st DOE/NRC Nuclear Air Cleaning Conference, San Diego, CA, pp. 271-298.

Haefner 2010 Haefner, D. R., and T. Watson, "Summary of FY 2010 Iodine Capture Studies at the INL," INL/EXT-10-19657, August 2010.

INL 2015 INL 2015, "Gaseous Fission Product Capture Testing," Laboratory Instruction (LI) 645, Idaho National Laboratory.

Jubin 2015 Jubin, R.T., B. B. Spencer, N. R. Soelberg, and D. M. Strachan, "Joint Test Plan to Identify the Gaseous By-Products of CH3I Loading on AgZ," Rev. 2, INL/EXT-12-27978, FCRD-SWF-2013-000070, ORNL/LTR-2012/604, November 30, 2015.

Law 2015 Law, J., N. Soelberg, T. Todd, J. Tripp (INL), C. Pereira, M. Williamson, W. Ebert (ANL), R. Jubin, B. Moyer (ORNL), J. Vienna, G. Lumetta, J. Crum (PNNL), T. Rudisill (SRNL), J. Bresee (DOE-NE), C. Phillips, B. Willis (EnergySolutions), P. Murray, S. Bader (AREVA), 2015, "Separation and Waste Form Campaign Full Recycle Case Study," FCRD-SWF-2013-000380, Revision 1, September 30.

Soelberg 2014 Soelberg, Nick and Tony Watson, "Phase 1 Methyl Iodide Deep-Bed Adsorption Tests," INL/EXT-14-32917, FCRD- SWF-2014-000271, August 22, 2014.

Soelberg 2015 Soelberg, Nick and Tony Watson, "FY-2015 Methyl Iodide Deep-Bed Adsorption Test Report," FCRD-MRWFD-2015-000267, INL/EXT-15-36817, Idaho National Laboratory, September 30, 2015.